

Accelerated Publications

Primary Reactions of the LOV2 Domain of Phototropin, a Plant Blue-Light Photoreceptor[†]

John T. M. Kennis,^{*,‡} Sean Crosson,[§] Magdalena Gauden,[‡] Ivo H. M. van Stokkum,[‡] Keith Moffat,^{§,||} and Rienk van Grondelle[‡]

Department of Biophysics, Faculty of Sciences, Vrije Universiteit, 1081 HV Amsterdam, The Netherlands, Department of Biochemistry and Molecular Biology, University of Chicago, Chicago, Illinois 60637, and Institute for Biophysical Dynamics, University of Chicago, Chicago, Illinois 60637

Received January 8, 2003; Revised Manuscript Received February 21, 2003

ABSTRACT: The phototropins constitute an important class of plant photoreceptor kinases that control a range of physiological responses, including phototropism, light-directed chloroplast movement, and light-induced stomatal opening. The LOV2 domain of phototropin binds a molecule of flavin mononucleotide (FMN) and undergoes a photocycle involving light-driven covalent adduct formation between a conserved cysteine residue and the C(4a) atom of FMN. This product state promotes C-terminal kinase activation and downstream signal transduction. Here, we report the primary photophysics and photochemistry of LOV2 domains of phototropin 1 of *Avena sativa* (oat) and of the phy3 photoreceptor of *Adiantum capillus-veneris* (maidenhair fern). In agreement with earlier reports [Swartz, T. E., et al. (2001) *J. Biol. Chem.* 276, 36493–36500], we find that the FMN triplet state is the reactive species from which the photoreaction occurs. We demonstrate that the triplet state is the primary photoproduct in the LOV2 photocycle, generated at 60% efficiency. No spectroscopically distinguishable intermediates precede the FMN triplet on the femtosecond to nanosecond time scale, indicating that it is formed directly via intersystem crossing (ISC) from the singlet state. Our results indicate that the majority of the FMN triplets in the LOV2 domain exist in the protonated form. We propose a reaction mechanism that involves excited-state proton transfer, on the nanosecond time scale or faster, from the sulfhydryl group of the conserved cysteine to the N5 atom of FMN. This event promotes adduct formation by increasing the electrophilicity of C(4a) and subsequent nucleophilic attack by the cysteine's thiolate anion. Comparison to free FMN in solution shows that the protein environment of LOV2 increases the ISC rate of FMN by a factor of 2.4, thus improving the yield of the cysteinyl–flavin adduct and the efficiency of phototropin-mediated signaling processes.

Plant growth and development are largely regulated by the light environment. Indeed, plants have evolved numerous

photoreceptors that are able to respond to both the blue and red regions of the visible spectrum (1, 2). The phototropin family of plant blue-light photoreceptors consists of serine/threonine kinases that undergo autophosphorylation in response to absorption of blue light (3), and control several physiological responses, including phototropism, light-mediated chloroplast movement, and stomatal opening (3–6). The loci for photochemistry in this class of photoreceptors are two flavin mononucleotide (FMN¹)-binding light, oxygen, or voltage (LOV) domains at the N-terminus of the protein (7). Each LOV domain consists of approximately 100 amino

[†] This work was supported by the Netherlands Organization of Scientific Research (NWO) through the council of Earth and Life Sciences (ALW) (J.T.M.K., M.G., and R.v.G.), the Foundation of Fundamental Research on Matter (FOM) (J.T.M.K.), NIH Grant GM 36452 to K.M., and an NSF Predoctoral Fellowship to S.C.

^{*} To whom correspondence should be addressed. E-mail: john@nat.vu.nl. Fax: +31 (0)204447999.

[‡] Vrije Universiteit.

[§] Department of Biochemistry and Molecular Biology, University of Chicago.

^{||} Institute for Biophysical Dynamics, University of Chicago.

acids and undergoes a self-contained photocycle, in which absorption of a blue photon leads to the formation of a long-lived species that absorbs at 390 nm (8–10). On the basis of the spectrum of a mutant form of mercuric reductase (11), it was proposed that this species corresponds to a covalent cysteinyl–C(4a) adduct (8). Recently, this intermediate has been directly confirmed using NMR spectroscopy and X-ray crystallography (12, 13), and by FTIR spectroscopy (14). Thus, absorption of blue light leads to the transient formation of a covalent bond between the FMN cofactor and the protein, which slowly disrupts to regenerate the noncovalent dark ground-state species.

The photoreaction of the *Avena sativa* LOV2 domain has been studied by means of nanosecond to second time-resolved absorption spectroscopy (10). These experiments indicate that the formation of a spectroscopic photointermediate denoted Phot^S₃₉₀, corresponding to the covalent FMN–cysteine adduct, takes place on a microsecond time scale. This species has a lifetime on the order of minutes before it returns to the ground state. An intermediate state preceding adduct formation, denoted Phot^L₆₆₀, exhibited spectral features characteristic of a FMN triplet state. On the basis of earlier molecular orbital calculations (15), this triplet state is the presumed reactive species that leads to adduct formation (9, 10).

The ability of a LOV domain to absorb a photon and to generate long-lived intermediate state(s) and a structural signal that affects autophosphorylation depends on very rapid, initial photochemical events that fix the energy of the singlet excited state of the protein-bound FMN chromophore. It is completely unknown how LOV domains transform the electronic energy of a photon into metastable species that enable signaling, and how the reaction is biased by specific FMN–protein interactions to produce a physiologically relevant state. Precedents from flavoenzymes and the flavin-binding DNA repair enzyme DNA photolyase suggest that light-induced electron transfer processes lie at the basis of these protein's photoreactivity (16–20). However, flavoenzymes differ fundamentally from LOV domains in that they do not have a light-activated function, and it cannot be expected *a priori* that the interactions between flavin and the protein environment exhibit any similarities. DNA photolyase does have a light-activated function, but utilizes a different redox state of the flavin cofactor (19, 20). To address the primary events of light activation in LOV domains, we have performed a femtosecond transient absorption study of the LOV2 domains of phot1 of *A. sativa* (oat) and of phy3 of *Adiantum capillus-veneris* (maidenhair fern), and of FMN in solution. Analysis of these ultrafast data for the LOV2 protein and comparison to free FMN in solution have allowed us to determine the primary photo-physical and photochemical events underlying cysteinyl–flavin adduct formation and subsequent phototropin-mediated signal transduction.

EXPERIMENTAL PROCEDURES

The LOV2 domain from *Ad. capillus-veneris* phy3 was expressed and purified as previously described (9). LOV2

from *A. sativa* phototropin 1 was expressed from a construct spanning residues 407–563 (construct generously provided by L. Neil and K. Gardner of the University of Texas Southwestern Medical Center, Dallas, TX), and contained an N-terminal fusion of protein G and a His tag. Twelve liters of cells was grown at 37 °C to an OD₆₀₀ of 0.4, induced with 500 μM isopropyl β-D-thiogalactoside, and grown for an additional 14 h after induction at 20 °C. Cells were lysed via sonication. *A. sativa* phot1 LOV2 was purified on Ni–NTA resin (Qiagen), and the fusion tag was cleaved with enterokinase (Boehringer-Mannheim). Anion exchange chromatography with high-performance Sepharose Q (Amersham Pharmacia) was used to separate the protease, cleaved protein, uncleaved protein, and N-terminal fusion peptide. Cleaved protein was concentrated in a high-pressure stirred ultrafiltration cell with a 3000 molecular weight cutoff filter (Amicon).

Prior to the experiments, LOV2 domains of *Adiantum* and *A. sativa* were dissolved in 20 mM Tris/150 mM NaCl buffer at pH 8.0. For the time-resolved experiments, the absorbance of the samples was adjusted to 0.3 mm⁻¹ at the absorption maximum. The samples were loaded in a flow system containing a cuvette with a path length of 1 mm, and flowed at a speed of approximately 5 cm/s by means of a peristaltic pump. The flow cuvette was mounted on a shaker that continuously vibrated the cuvette sideways at a frequency of 20 Hz with an amplitude of 1 mm. For the fluorescence measurements, the samples were diluted to an absorbance of 0.05 cm⁻¹, and contained in quartz cuvettes with a path length of 1 cm. FMN was purchased from Sigma Chemicals and used without further purification. FMN was dissolved in 20 mM Tris, acetate, or formate buffer at pH 8.0, 5.0, or 2.0, respectively.

Steady-state absorption spectra were recorded on a commercial spectrometer (Perkin-Elmer). Fluorescence spectra were recorded with a commercial fluorimeter (Perkin-Elmer) with a right-angle detection geometry. The samples were excited at 445 nm at an excitation power of 15 μW at a beam diameter of 0.5 cm². The fluorescence quantum yield of LOV2 was determined by recording the fluorescence spectra of LOV2 and FMN in aqueous buffer at pH 8.0 under identical conditions. The number of absorbed photons was taken into account by correcting for the sample transmission. The fluorescence quantum yield of FMN in water, 0.26, has been previously determined (21).

Femtosecond transient absorption spectroscopy was carried out with an amplified Ti:sapphire laser system (Coherent/BMI), operating at 1 kHz, equipped with a home-built noncollinear optical parametric amplifier (NOPA), described in detail previously (22). The output of the NOPA was tuned to 475 nm, attenuated to 350 or 700 nJ, and used as a pump beam. A white-light continuum was generated by focusing the rest of the output of the regenerative amplifier at 800 nm on a 1 mm sapphire crystal, and split into probe and reference beams. The pump beam from the NOPA and the probe beam were focused on the sample cuvette at a spot with a diameter of 150 μm. Femtosecond time delays between the pump and probe were controlled by a delay line covering delays up to 8 ns. The pump and probe were polarized at the magic angle (54.7°). After passing through the sample, the probe and reference beams were dispersed

¹ Abbreviations: FMN, flavin mononucleotide; LOV, light, oxygen, or voltage; ISC, intersystem crossing; IC, internal conversion; SADS, species-associated difference spectrum.

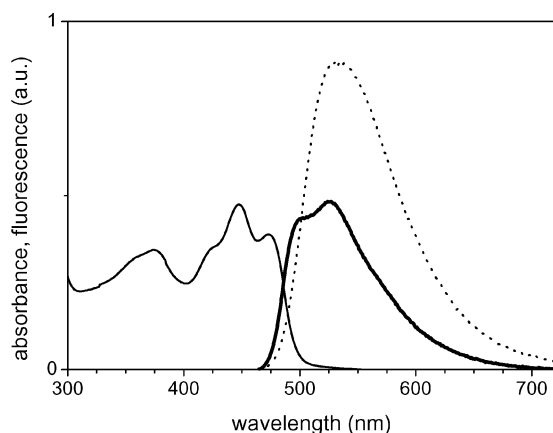


FIGURE 1: Absorption spectrum of the LOV2 domain of phy3 of *Ad. capillus-veneris* (thin solid line), fluorescence spectrum of FMN in aqueous buffer at pH 8.0 (dotted line) with excitation at 450 nm, and fluorescence spectrum of the phy3 LOV2 domain of *Ad. capillus-veneris* (thick solid line). The spectra have been scaled to equal numbers of absorbed photons.

by a polychromator and projected on a double-diode array detector.

The time-resolved spectra were analyzed with a global analysis program using a kinetic model consisting of sequentially interconverting species, i.e., $1 \rightarrow 2 \rightarrow 3 \rightarrow \dots$ (23), in which the arrows indicate successive monoexponential decays of increasing time constants, which can be regarded as the lifetime of each species. Associated with each species are a lifetime and a difference spectrum, denoted the species-associated difference spectrum (SADS). The first SADS corresponds to the time-zero difference spectrum. In general, the SADS may well correspond to mixtures of excited states and does not necessarily portray spectra of pure states. This procedure enables us to visualize clearly the evolution of the (excited) states of the system. The instrument response function was fit to a Gaussian (120 fs full width at half-maximum). To illustrate our observations optimally, we present them in the form of SADS instead of raw time-resolved spectra.

RESULTS AND DISCUSSION

Steady-State Spectroscopy

Figure 1 shows the absorption spectrum of the LOV2 domain of *Adiantum* phy3 (thin solid line). The lowest singlet excited state, S_1 , of the protein-bound FMN chromophore absorbs maximally around 450 nm and shows a vibronic progression with features at 422, 447, and 474 nm. The short-wavelength band at 375 nm can be assigned to the higher-lying S_2 singlet excited state of FMN.

The steady-state fluorescence spectra of LOV2 and FMN in aqueous solution upon excitation at 445 nm are also shown in Figure 1. The LOV2 fluorescence spectrum (thick solid line) shows vibronic structure with features at 500 and 528 nm. The fluorescence spectrum of FMN in aqueous buffer (dotted line) is featureless with a single maximum at 530 nm. To assess the loss of FMN singlet states in the LOV2 domain by radiative decay, we determined the fluorescence quantum yield. The fluorescence spectra of FMN and LOV2 in Figure 1 are depicted with an equal number of absorbed photons. The wavelength-integrated fluorescence of LOV2

amounts to half that of FMN in solution. Given a fluorescence quantum yield of 0.26 in FMN in solution (21), the fluorescence quantum yield in LOV2 is 0.13. This number is similar to that obtained recently for the LOV1 domain of phototropin from *Chlamydomonas reinhardtii*, namely, 0.17 (24).

Time-Resolved Spectroscopy

Free FMN. To compare of the properties of the free FMN chromophore with those of FMN bound to the LOV2 domain, we performed femtosecond transient absorption measurements on FMN dissolved in aqueous buffer. The sample was excited at 475 nm, and the time-resolved absorbance changes were monitored over a wavelength range from 520 to 750 nm. Figure 2A shows the results at pH 5.0 in the form of a global analysis of the data. Three components were required for an adequate description of the time-resolved data, with lifetimes of 1.6 ps and 4.7 ns and a component that did not decay on the time scale of our experiment. Each species is characterized by a species-associated difference spectrum, SADS, relative to the ground-state absorption, and by a rise time and a decay time. The dotted line in Figure 2A represents the initial absorption change, determined from the raw data after correction for the group velocity dispersion in the probe light and deconvolution with the instrument response function. This SADS, which can be assigned to the initially created singlet excited state of FMN, shows a pronounced stimulated emission band near 570 nm and a broad excited-state absorption at wavelengths longer than 650 nm. At wavelengths shorter than 530 nm, the signal is dominated by excited-state absorption. The initially created state evolves into the second state (thin solid line) in 1.6 ps. The SADS of this state exhibits a small red shift of the stimulated emission. The 1.6 ps evolution may be assigned to the diffusive component of a solvation process, i.e., a dynamic rearrangement of water molecules around the newly created singlet excited state of FMN (25). This “relaxed” FMN singlet excited state evolves in 4.7 ns into the third state (thick solid line), which does not decay on the time scale of the experiment. A singlet excited-state lifetime of 4.7 ns of free FMN agrees well with that published in the literature (24, 26). The SADS of this final state shows a broad excited-state absorption, with two distinct maxima at 650 and 710 nm and a minimum near 530 nm. These spectral characteristics agree with that of the FMN triplet state at neutral pH values (10, 27, 28). Time-resolved measurements on FMN dissolved in aqueous buffer at pH 8.0 and 10.0 showed results very similar to those in Figure 2A (not shown). To illustrate the quality of the time-resolved data and the global analysis, a kinetic trace at 560 nm of FMN at pH 5.0 is shown in Figure 2E (circles), along with the result of the analysis procedure (solid line).

Previous experiments on FMN at nanosecond to microsecond time scales have indicated that at acidic pH, protonation of the FMN triplet state takes place, presumably at N5 of the isoalloxazine ring (28). Because protonation of this nitrogen may be a prerequisite for adduct formation in the LOV2 photocycle (9, 10), we investigated these excited-state proton transfer processes in free FMN. Figure 2B shows the results of a global analysis of time-resolved measurements on FMN in aqueous buffer at pH 2.0. Three components are necessary for a satisfactory description of the time-resolved

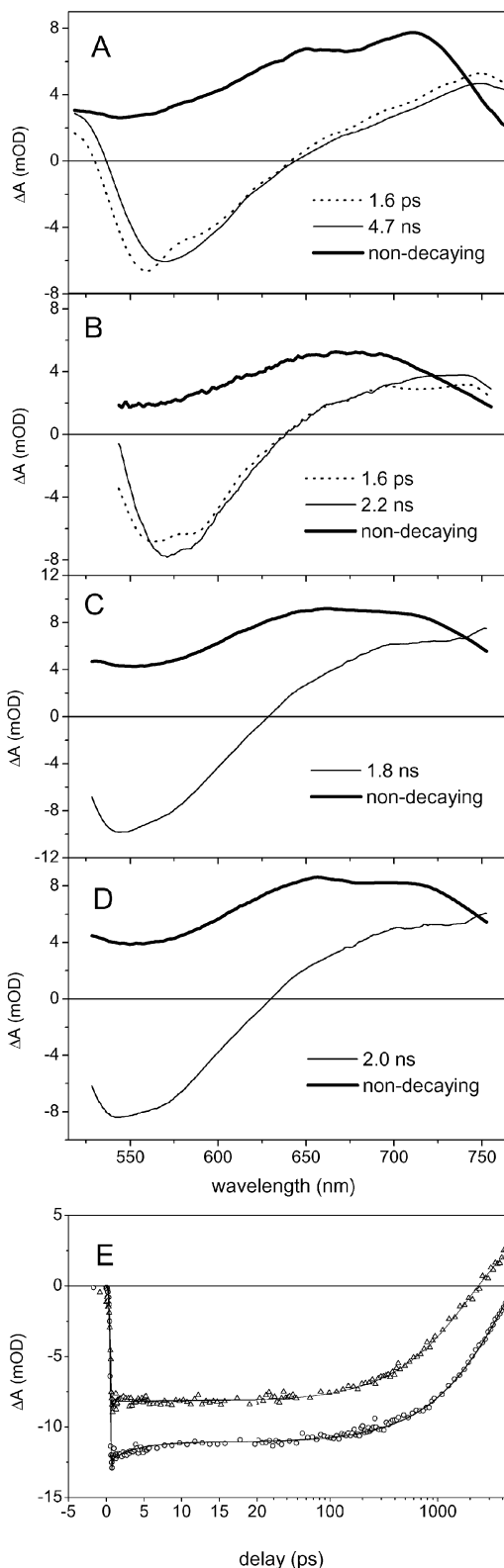


FIGURE 2: Species-associated difference spectra (SADS) and associated lifetimes that result from a global analysis procedure on time-resolved measurements upon excitation at 475 nm. (A) FMN dissolved in aqueous buffer at pH 5.0. (B) FMN dissolved in aqueous buffer at pH 2.0. (C) Same as for panel A for the phy3 LOV2 domain of *Ad. capillus-veneris* (fern). (D) Same as for panel A for the phot1 LOV2 domain of *A. sativa* (oat). (E) Kinetic trace at 560 nm recorded in FMN in aqueous buffer at pH 5.0 (\circ) and of LOV2 of *A. sativa* at 530 nm (Δ). The solid lines denote the results of the global analysis procedure. Note that the time axis is linear from -5 to 20 ps, and logarithmic thereafter.

data, with time constants of 1.6 ps and 2.2 ns and a nondecaying component. The initial two SADS are very similar to those at pH 5.0 (Figure 2A) and can be assigned to the unrelaxed and relaxed FMN singlet excited states. The singlet excited-state lifetime of 2.2 ns is significantly shorter than that at neutral pH. The SADS of the nondecaying component, which we assign to the FMN triplet state, differs from that at pH 5.0 in that it exhibits a single broad maximum at 675 nm, and is overall blue-shifted. The amplitude of the triplet spectrum is notably lower than at pH 5, which indicates that the triplet yield may be lower than at neutral pH.

The difference spectra reported by Sakai and Takahashi (28) for the FMN triplet state in the protonated (pH 3.2) and unprotonated form (pH 5–8) agree well with the nondecaying SADS shown in panels A and B of Figure 2. Our measurements thus show that at pH 2, excited-state proton transfer takes place from the buffer solution to FMN on a time scale of nanoseconds or faster. We do not observe a specific spectral evolution associated with the protonation event. This means either that protonation takes place in the triplet state but that the intersystem crossing (ISC) process is rate-limiting and the unprotonated triplet escapes detection or that protonation takes place in the singlet state but is not associated with distinct spectral changes in this state. Moreover, it is not clear at present whether the shortening of the FMN singlet-state lifetime at pH 2 to 2.2 ns arises from an enhanced rate of internal conversion (IC) to the ground state that results from protonation of the singlet state, or from a proton collisional quenching mechanism, after which protonation of the remaining FMN triplet states occurs.

LOV2 Domains. We performed femtosecond time-resolved absorption spectroscopy on the LOV2 domain of *Adiantum* phy3 and *A. sativa* phot1 to assess the primary photophysical and photochemical events that eventually lead to formation of the covalent adduct between the FMN chromophore and cysteine. The samples were excited at 475 nm, at the low-energy side of the S_1 state of the FMN chromophore. Figure 2C shows the results for the LOV2 domain of *Adiantum* phy3. Global analysis of the time-resolved data indicated that two components are sufficient for an adequate description. The SADS of the initially created singlet excited state of the protein-bound FMN chromophore (thin line) exhibits spectral properties that are similar to those of FMN in solution, with a stimulated emission band around 530 nm and a pronounced excited-state absorption at wavelengths longer than 625 nm. The initially created singlet excited state evolves into the final state in 1.8 ns (thick line), which does not decay on the time scale of the experiment. This final SADS shows an excited-state absorption at all wavelengths and has a broad maximum near 650 nm, a shoulder near 710 nm, and a shallow minimum near 550 nm.

Figure 2D shows the results for the LOV2 domain of *A. sativa* phot1. They are very similar to those obtained for *Adiantum*, with similar SADS for the initial (thin line) and final (thick line) absorption changes of protein-bound FMN, and a singlet excited-state lifetime of 2.0 ns. The kinetic trace at 530 nm of *A. sativa* LOV2 is shown in Figure 2E, along with the result of the global analysis. These lifetimes of LOV2 domains, 1.8 and 2.0 ns, are somewhat shorter than that reported for the LOV1 domain of *C. reinhardtii*, 2.9 ns (24).

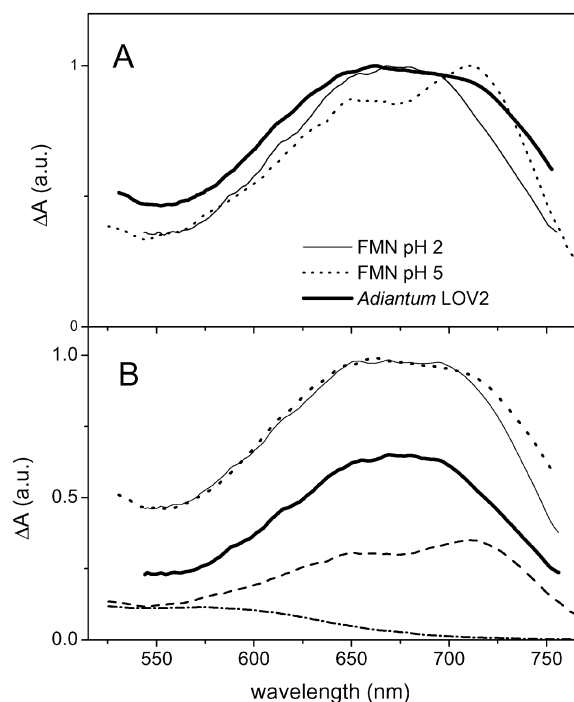


FIGURE 3: (A) Nondecaying species-associated difference spectra of *Adiantum* phy3 LOV2 (thick solid line), reproduced from Figure 2C, and of FMN at pH 5 (dotted line) and pH 2 (thin solid line), reproduced from panels A and B of Figure 2, respectively, normalized at their respective maxima. (B) Difference spectra of the protonated (thick solid line) and unprotonated (dashed line) free FMN triplet spectra and of the semiquinone of FMN (dashed and dotted line) taken from ref 26, plotted in a stoichiometric amplitude ratio of 6:3:1, corrected for their respective extinction coefficients. The thin solid line is a sum of the protonated, unprotonated, and semiquinone FMN spectra in this ratio. The dotted line is the nondecaying SADS of *Adiantum* LOV2.

Figure 3A reproduces the nondecaying SADS of FMN at pH 5.0 and 2.0, and of *Adiantum* LOV2 from panels A–C of Figure 2, normalized at their maxima. The broad excited-state absorption features in the final SADS of LOV2 domains near 650–710 nm are indicative of the FMN triplet state. Moreover, the final SADS of LOV2 closely resembles the difference spectrum assigned to the $\text{Phot}^{\text{L}}_{660}$ intermediate, reported by Swartz et al. for *A. sativa* phot1 LOV2 (10). On the other hand, the difference spectra of the FMN semiquinone neutral radical and radical cation spectra are very dissimilar to the final LOV2 SADS (10, 28). Thus, the final state in the LOV2 domain on a nanosecond time scale can primarily be assigned to the triplet state of the protein-bound FMN chromophore. We conclude that the early events in the LOV2 domain after photoexcitation involve direct evolution from the FMN singlet excited state to the FMN triplet state. Since we do not observe any intermediate states, ISC of the singlet excited state is the most likely mechanism by which triplet formation proceeds. Our results exclude a mechanism for triplet formation by which a light-induced charge-separated state (for instance, as a result of electron transfer from tryptophan or tyrosine residues to FMN; see refs 16–18) recombines on the nanosecond time scale to form the triplet state. Such a radical-pair mechanism is for instance in effect in photosynthetic reaction centers, where, under the right circumstances, it can result in (bacterio)chlorophyll triplet yields of up to 100% (29).

The steady-state absorption and fluorescence bands of the LOV2 domain are narrower and show more structure than those of FMN in water, which indicates a nonpolar, ordered environment around the FMN chromophore in the protein. Similar narrow and resolved absorption bands could be expected for the LOV2 triplet state. However, we observe the opposite: the LOV2 triplet absorption band is significantly broader than those of FMN in water in either its protonated or unprotonated form, as can be seen in Figure 3A. This indicates that the LOV2 triplet exists as a heterogeneous species, possibly as a mixture of protonated and unprotonated forms. In Figure 3B, we have described the nondecaying SADS of the LOV2 domain (dotted line) in terms of a superposition of the difference spectra of the protonated (thick solid line) and unprotonated (dashed line) free FMN triplet spectra of panels B and A of Figure 2, and a minor contribution by the semiquinone form of FMN (dashed and dotted line), taken from ref 28. A superposition of the spectra of these species in a stoichiometric ratio of 6:3:1, corrected for their extinction coefficients, yields the thin solid curve, which accurately describes the LOV2 spectrum in the spectral region from 540 to 710 nm. The deviation at wavelengths of >710 nm may result from a slight red-shifted absorption of the FMN triplet state in the protein as compared to that in solution. Thus, on the nanosecond time scale, the majority of FMN triplet states in the LOV2 domain exist in the protonated form. As with free FMN in aqueous solution at pH 2, we do not observe a specific spectral evolution that can be associated with the excited-state protonation event, which implies that excited-state proton transfer either takes place in the triplet state in a fashion that is rate-limited by the ISC process, or already has taken place in the singlet excited state. Moreover, these results indicate that light-induced electron transfer processes, if they occur at all, have a yield of less than 10% in the LOV2 domain.

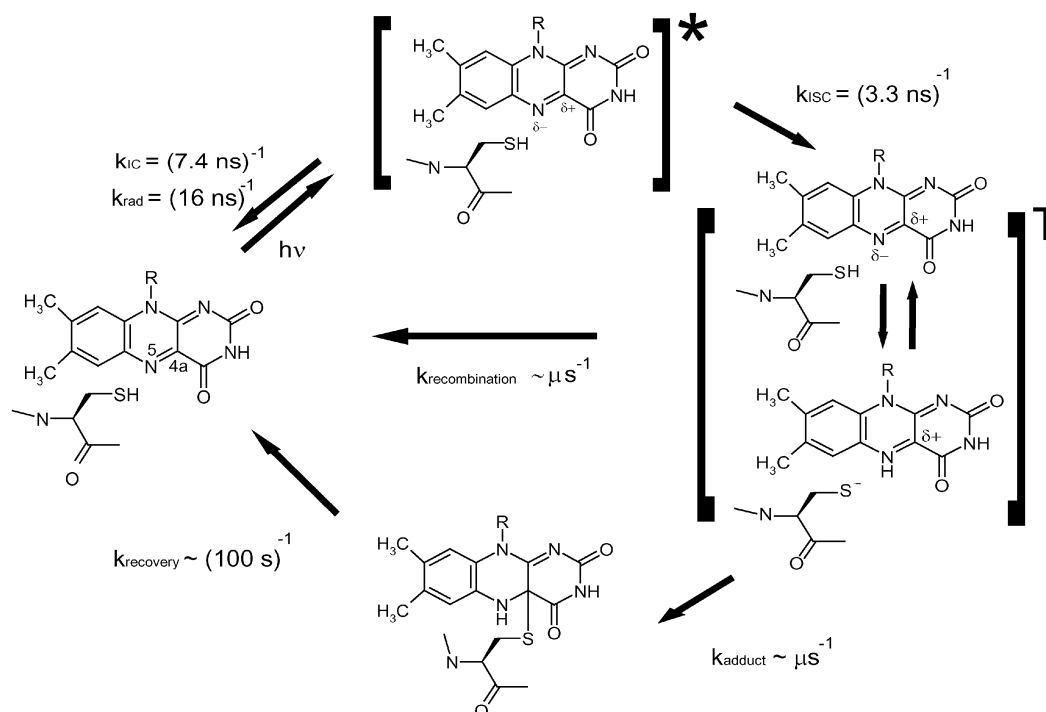
Reaction Yields in the LOV2 Domain

The amplitude of the triplet spectrum of the LOV2 domain with respect to the amplitude of the stimulated emission band of the LOV2 singlet excited state is a measure of the triplet yield in the LOV domain; it may be compared with the corresponding spectra of the FMN chromophore in solution, for which the triplet yield is known to be 0.6 at neutral pH values (30). We assume that the (difference) extinction coefficients for singlet ground-state absorption, and thus for stimulated emission, and for the triplet excited-state absorption are identical in LOV2 and FMN in solution. It is reasonable to assume that the triplet extinction coefficients of protonated and unprotonated FMN chromophores are similar at their respective maxima. The apparently lower triplet yield at pH 2.0 (Figure 2B) then is consistent with the shorter singlet excited-state lifetime of 2.2 ns, and arises from an enhanced IC rate.

We find that the amplitudes of the triplet excited-state absorption near 660 nm with respect to the stimulated emission signal at 530 nm in the LOV2 domains of both *Adiantum* and *A. sativa* (as observed in the final and first SADS in panels C and D of Figure 2, respectively) are basically the same as the corresponding quantities of FMN in solution at pH 5.0 measured near 670 and 570 nm (final and second SADS in Figure 2A, respectively). We conclude

Table 1: Fluorescence Lifetimes (τ_{fl}) and Yields (Φ_F), Triplet Yields (Φ_T), Rates of ISC (k_{ISC}) and IC (k_{IC}), and Radiative Rates (k_{rad}) in the Free FMN Chromophore at Neutral pH, and of FMN Bound to LOV2 Domains

	τ_{fl} (ns)	Φ_T	Φ_F	k_{ISC}	k_{IC}	k_{rad}
free FMN at neutral pH	4.7	0.6	0.26	$(7.8 \text{ ns})^{-1}$	$(34 \text{ ns})^{-1}$	$(18 \text{ ns})^{-1}$
LOV2	2.0	0.6	0.13	$(3.3 \text{ ns})^{-1}$	$(7.4 \text{ ns})^{-1}$	$(16 \text{ ns})^{-1}$

Scheme 1: Photocycle of the LOV2 Domain, with the Photophysical and Photochemical Reaction Rates Indicated at the Arrows^a

^a The positions of the catalytically important C(4a) and N5 atoms of the isoalloxazine ring have been indicated in the ground-state FMN at the left side. See the text for further details.

that the triplet yield of the LOV2 domains of *Adiantum* phy3 and *A. sativa* phot1 is very similar to that of FMN in solution, i.e., 0.6. This number is lower than that reported by Swartz et al. for the phot1 LOV2 domain of *A. sativa* (10). They estimated an initial triplet yield after photoexcitation of 0.88, of which 50% led to adduct formation and 50% returned to the ground state, resulting in a final covalent adduct yield of 0.44. Recent estimates for a variety of LOV2 domains gave adduct quantum yields of around 0.3 (31), which is in line with the findings presented here.

After photoexcitation of the FMN chromophore to its singlet excited state, the efficiency of the LOV2 photoreaction is determined by competition between ISC to the triplet state, occurring at a rate k_{ISC} , loss processes such as radiative decay (fluorescence) to the ground state at a rate k_{rad} , and internal conversion (IC) to the ground state at a rate k_{IC} . As we argued above, other loss processes such as electron transfer have a small yield of $\leq 10\%$ in LOV2. If they occur at all, they are unlikely to be physiologically relevant and can formally be incorporated in the IC loss channel. In FMN in aqueous solution, the triplet and fluorescence yields Φ_T and Φ_F are 0.6 and 0.26, respectively (21, 30). The corresponding values in *Adiantum* phy3 LOV2 and *A. sativa* phot1 LOV2 are 0.6 and 0.13, respectively. By using the singlet excited-state lifetimes of 4.7 ns for FMN in solution and 2.0 ns for LOV2, we can now determine the rate

constants k_{ISC} , k_{IC} , and k_{rad} in these systems. We find that $k_{ISC} = (7.8 \text{ ns})^{-1}$ in FMN and $(3.3 \text{ ns})^{-1}$ in LOV2. Furthermore, $k_{IC} = (34 \text{ ns})^{-1}$ in FMN and $(7.4 \text{ ns})^{-1}$ in LOV2. As may be expected on the basis of the similar extinction coefficients of FMN in solution and in LOV2, the radiative rates are nearly identical: $k_{rad} = (18 \text{ ns})^{-1}$ for FMN and $(16 \text{ ns})^{-1}$ in LOV2. It follows that the ISC rate is enhanced in the LOV2 domain as compared to FMN in solution by a factor of 2.4. A similar conclusion was drawn for the LOV1 domain of *Chlamydomonas* on the basis of time-resolved fluorescence results (24). The enhancement may be ascribed to the presence of the cysteine sulfur near the flavin isoalloxazine ring. It thus appears, intriguingly, that the proximity of the cysteine to the isoalloxazine ring not only provides the structure that enables formation of a covalent adduct but also facilitates the rapid electronic formation of the reactive FMN triplet state. The overall yield of the cystenyl-flavin C(4a) adduct is thereby maximized. The values for the various rate constants in the LOV2 domain and free FMN have been summarized in Table 1.

Reaction Mechanism of Adduct Formation in LOV2

Our experiments clearly indicate that the FMN triplet state is the reactive species in the LOV2 photocycle from which adduct formation proceeds directly. Moreover, our observations indicate that on the nanosecond time scale, the majority

of the FMN triplet states exist in the protonated form. Quantum chemical calculations have indicated that upon excitation of flavin to the singlet or triplet excited state, the basicity of the N1 atom of the isoalloxazine ring decreases, while that of N5 increases (15, 32), indicating that protonation most likely takes place at N5. These protons may originate from the thiol of the conserved cysteine, considering its favorable position with respect to the isoalloxazine ring (9). This invokes a reaction mechanism that involves base abstraction of the thiol proton by the excited FMN chromophore. This, in turn, would increase the electrophilicity of C(4a) and promote nucleophilic attack of the thiolate anion at this position to form the adduct (9).

Notably, in a mutant of the homologous LOV1 domain of *Chlamydomonas*, which lacked the conserved cysteine, the transient absorption spectrum of the triplet state exhibited a double band structure at 660 and 720 nm (33), similar to that of free FMN at pH 5.0 shown in Figure 2A, whereas the wild-type LOV1 domain exhibited a single broad maximum near 670 nm, similar to the LOV2 triplet spectrum shown in panels C and D of Figure 2. Although not interpreted as such by the authors, these observations support our idea that the triplet state in the LOV domain is protonated, and that the proton originates from the conserved cysteine's thiol group.

From the LOV2 triplet state, ~50% returns to the ground state without forming an adduct (10). The extent of protonation of the FMN chromophore on the nanosecond time scale may already define the branching ratio between recombination and adduct formation. Titration experiments of the phot1 LOV2 domain of *A. sativa* have indicated that the conserved cysteine may exist as a thiolate ($-S^-$) in the ground state (10). On the other hand, recent FTIR experiments have unequivocally demonstrated that at least a significant fraction of the cysteine exists in the thiol ($-SH$) conformation (34). It is conceivable that in the ground state, LOV2 domains actually exist as a heterogeneous mixture of thiol and thiolate conformers, which may correlate with the partial protonation of the FMN triplet state upon photon absorption and the subsequent branching of the photoreaction.

Scheme 1 summarizes our results and the implications for the mechanism of the light-induced reaction in the LOV2 domain. Upon photoexcitation to the FMN singlet excited state, the triplet state is formed through ISC with a yield of 0.6. In competition with ISC, radiative decay and IC to the ground state take place with yields of 0.13 and 0.27, respectively. Excited-state proton transfer on the nanosecond time scale or faster, presumably from the conserved cysteine to the N5 atom of the FMN chromophore, may represent an important primary event that may trigger the formation of the covalent adduct. Although in Scheme 1 the protonation state of the FMN triplet has been indicated as an equilibrium between protonated and unprotonated species, it not clear at present what underlies the observed heterogeneity, and it might well correspond to a static distribution rather than a dynamic equilibrium. Moreover, the excited-state proton transfer process may well take place in the FMN singlet excited state rather than in the triplet state. From the FMN triplet state, the covalent adduct is formed with a probability of ~50% (10), which implies that the total quantum yield of the LOV2 photocycle is 0.3.

CONCLUSIONS

The primary photophysical and photochemical reactions in the LOV2 domain of plant blue-light photoreceptors are relatively simple, and involve intersystem crossing from the singlet excited state of the FMN chromophore to the triplet excited state, accompanied by an excited-state proton transfer from the conserved cysteine's thiol to FMN. No further spectroscopically distinguishable intermediates precede the subsequent formation of a covalent adduct on a microsecond time scale.

LOV domains exhibit a unique photoreaction behavior among flavoproteins, which often exhibit rapid and efficient electron transfer processes on light absorption (16–20). In LOV domains, electron transfer processes are not required because the charges required for adduct formation are already present between the isoalloxazine ring of FMN and the cysteine side chain. Instead, the electronic excited state of FMN is stabilized by the protein environment, and ISC to the triplet state, enhanced by the presence of the cysteine near the isoalloxazine ring, provides for a crucially extended time window in which efficient adduct formation can proceed.

ACKNOWLEDGMENT

The constructs of maidenhair fern phy3 LOV2 and oat phot1 LOV2 were generously provided by John Christie and Winslow Briggs of the Carnegie Institution of Washington (Stanford, CA) and Lori Neil and Kevin Gardner of the University of Texas Southwestern Medical Center, respectively.

REFERENCES

1. Briggs, W. R., and Huala, E. (1999) *Annu. Rev. Cell Dev. Biol.* 15, 33–62.
2. Fankhauser, C., and Chory, J. (1999) *Curr. Biol.* 9, 123–126.
3. Christie, J. M., Reymond, P., Powell, G. K., Bernasconi, P., Raibekas, A. A., Liscum, E., and Briggs, W. R. (1998) *Science* 282, 1698–1701.
4. Huala, E., Oeller, P. W., Liscum, E., Han, I.-S., Larsen, E., and Brigs, W. R. (1997) *Science* 278, 2120–2123.
5. Kagawa, T., Sakai, T., Suetsugu, N., Oikawa, K., Ishiguro, S., Kato, T., Tabata, S., Okada, K., and Wada, M. (2001) *Science* 291, 2138–2141.
6. Kinoshita, T., Michio Doi, M., Suetsugu, N., Kagawa, T., Wada, M., and Shimazaki, K.-I. (2001) *Nature* 414, 656–660.
7. Christie, J. M., Salomon, M., Nozue, K., Wada, M., and Briggs, W. R. (1999) *Proc. Natl. Acad. Sci. U.S.A.* 96, 8779–8783.
8. Salomon, M., Christie, J. M., Knib, E., Lempert, U., and Briggs, W. R. (2000) *Biochemistry* 39, 9401–9410.
9. Crosson, S., and Moffat, K. (2001) *Proc. Natl. Acad. Sci. U.S.A.* 98, 2995–3000.
10. Swartz, T. E., Corchnoy, S. B., Christie, J. M., Lewis, J. W., Szundi, I., Briggs, W. R., and Bogomolni, R. A. (2001) *J. Biol. Chem.* 276, 36493–36500.
11. Miller, S. M., Massey, V., Ballou, D., Williams, C. H., Distefano, M. D., Moore, M. J., and Walsh, C. T. (1990) *Biochemistry* 29, 2831–2841.
12. Crosson, S., and Moffat, K. (2002) *Plant Cell* 14, 1067–1075.
13. Salomon, M., Eisenreich, W., Durr, H., Schleicher, E., Knieb, E., Massey, V., Rudiger, W., Muller, F., Bacher, A., and Richter, G. (2001) *Proc. Natl. Acad. Sci. U.S.A.* 98, 12357–12361.
14. Swartz, T. E., Wenzel, P. J., Corchnoy, S. B., Briggs, W. R., and Bogomolni, R. A. (2002) *Biochemistry* 41, 7183–7189.
15. Song, P. S. (1968) *Photochem. Photobiol.* 7, 311–313.
16. Van den Berg, P. A. W., and Visser, A. J. W. G. (2001) in *New Trends in Fluorescence Spectroscopy: Applications to Chemical and Life Sciences* (Valeur, B., and Brochon, J.-C., Eds.) p 457, Springer, New York.

17. Mataga, N., Chosrowjan, H., Shibata, Y., Tanaka, F., Nishina, Y., and Shiga, K. (2000) *J. Phys. Chem. B* 104, 10667–10677.
18. Zhong, D. P., and Zewail, A. H. (2001) *Proc. Natl. Acad. Sci. U.S.A.* 98, 11867–11872.
19. Sancar, A. (1994) *Biochemistry* 33, 2–9.
20. Aubert, C., Vos, M. H., Mathis, P., Eker, A. P. M., and Brettel, K. (2000) *Nature* 405, 586–590.
21. Weber, G. (1950) *Biochem. J.* 47, 114.
22. Gradinaru, C. C., Kennis, J. T. M., Papagiannakis, E., van Stokkum, I. H. M., Cogdell, R. J., Fleming, G. R., Niederman, R. A., and van Grondelle, R. (2001) *Proc. Natl. Acad. Sci. U.S.A.* 98, 2364–2369.
23. Van Stokkum, I., Scherer, T., Brouwer, A., and Verhoeven, J. (1994) *J. Phys. Chem.* 98, 852–866.
24. Holzer, W., Penzkofer, A., Fuhrmann, M., and Hegemann, P. (2002) *Photochem. Photobiol.* 75, 479.
25. Jimenez, R., Fleming, G. R., Kumar, P. V., and Maroncelli, M. (1994) *Nature* 369, 471–473.
26. Visser, A. J. W. G., Van Hoek, A., Visser, N. W., Lee, Y., and Ghisla, S. (1997) *Photochem. Photobiol.* 65, 570–575.
27. Heelis, P. F., Parsons, B. J., Phillips, G., and McKellar, J. (1978) *Photochem. Photobiol.* 28, 169–173.
28. Sakai, M., and Takahashi, H. (1996) *J. Mol. Struct.* 379, 9–18.
29. Hoff, A. J. (1996) in *Biophysical Techniques in Photosynthesis* (Amesz, J., and Hoff, A. J., Eds.) p 209, Kluwer Academic Publishers, Dordrecht, The Netherlands.
30. Heelis, P. F. (1991) in *Chemistry and biochemistry of flavoenzymes* (Muller, F., Ed.) Vol. I, p 171, CRC Press, Boca Raton, FL.
31. Kasahara, M., Swartz, T., Olney, M., Onodera, A., Mochizuki, N., Fukuzawa, H., Asamizu, E., Tabata, S., Kanegae, H., Takano, M., Christie, J. M., Nagatani, A., and Briggs, W. R. (2002) *Plant Physiol.* 129, 762–773.
32. Martin, C. B., Tsao, M.-L., Hadad, C. M., and Platz, M. S. (2002) *J. Am. Chem. Soc.* 124, 7726–7734.
33. Kottke, T., Heberle, J., Hehn, D., Dick, B., and Hegemann, P. (2003) *Biophys. J.* 84, 1192–1201.
34. Iwata, T., Tokutomi, S., and Kandori, H. (2002) *J. Am. Chem. Soc.* 124, 11840–11841.

BI034022K